



## Obrabotka metallov -

## Metal Working and Material Science

Journal homepage: [http://journals.nstu.ru/obrabotka\\_metallov](http://journals.nstu.ru/obrabotka_metallov)




### Integrated numerical and experimental investigation of tribological performance of PTFE based composite material



Abhijeet Deshpande<sup>1, a, \*</sup>, Atul Kulkarni<sup>2, b</sup>, Prashant Anerao<sup>2, c</sup>,  
 Leena Deshpande<sup>1, d</sup>, Avinash Somatkar<sup>1, e</sup>

<sup>1</sup> Vishwakarma Institute of Information Technology, Survey No. 3/4, Kondhwa (Budruk), Maharashtra, Pune - 411048, India

<sup>2</sup> Vishwakarma Institute of Technology, Pune, Maharashtra, 411037, India

<sup>a</sup>  <https://orcid.org/0000-0001-8956-3093>,  [abhijeet.deshpande@vit.ac.in](mailto:abhijeet.deshpande@vit.ac.in); <sup>b</sup>  <https://orcid.org/0000-0002-6452-6349>, [atul.kulkarni@vit.edu](mailto:atul.kulkarni@vit.edu);

<sup>c</sup>  <https://orcid.org/0000-0003-0353-7420>,  [prashant.anerao@vit.edu](mailto:prashant.anerao@vit.edu); <sup>d</sup>  <https://orcid.org/0000-0001-7426-2028>,  [leena.deshpande@vit.ac.in](mailto:leena.deshpande@vit.ac.in);

<sup>e</sup>  <https://orcid.org/0000-0002-2885-2104>,  [avinash.somatkar@vit.ac.in](mailto:avinash.somatkar@vit.ac.in)

#### ARTICLE INFO

##### Article history:

Received: 22 January 2025

Revised: 17 February 2025

Accepted: 27 March 2025

Available online: 15 June 2025

##### Keywords:

Green manufacturing

Composite and sustainability

FEA

Glass

Carbon

PTFE

Wear behavior

#### ABSTRACT

**Introduction.** One of the most significant phenomena in every industrial sector is friction and wear, which inevitably occurs when there is relative motion between similar or dissimilar materials. A substantial portion of global energy production is estimated to be expended in overcoming friction and wear, making them critical factors in energy efficiency and sustainability. Recently, advances in materials science, lubrication technologies, and innovative design approaches have facilitated a significant reduction in friction and wear, leading to considerable energy savings and extended component lifespan. Polytetrafluoroethylene (PTFE), among other materials, has revolutionized the tribological field, emerging as a highly effective synthetic polymer. This is attributed to its exceptional properties, including a low coefficient of friction, chemical inertness, thermal stability, non-stick characteristics, and biocompatibility. These unique properties make PTFE an ideal material for various industrial applications, spanning from aerospace to biomedical sectors. **The purpose of work.** This study aims to conduct a comprehensive numerical and experimental investigation into the tribological properties of PTFE-based composites. The materials selected for investigation include pure PTFE, PTFE with 25% carbon (C) filler, and PTFE with 20% glass filler. Testing was performed using stainless steel (SS 304) as the counterbody. Tribological testing and subsequent evaluation were conducted under dry sliding friction conditions, considering key parameters such as load, sliding speed, and temperature. Response surface methodology (RSM) was employed to develop an empirical model, utilizing experimental data to predict the wear resistance of these materials. Empirical models were developed to understand the influence of process parameters on wear behavior and to optimize operating conditions for minimizing material loss. **Method of investigation.** Archard's wear model was used as the theoretical framework for predicting volume loss and specific wear rate based on numerical simulations. The wear coefficient (K) was determined through experimental testing and used as an input parameter in the numerical models. Numerical simulations were developed using the finite element analysis (FEA) software ANSYS, enabling the simulation of complex tribological interactions between the composite materials and the counterbody. A central composite rotatable design (CCRD) within the framework of RSM was used to structure the experiments. The experiments were conducted under dry sliding friction conditions using pin on disc tribometer. The input parameters for the experiments were load (ranging from 15 N to 200 N), sliding speed (ranging from 400 rpm to 1000 rpm), and temperature (ranging from 60 °C to 200 °C). Each experiment was conducted for a sliding distance of 5 km to ensure sufficient wear for analysis. A total of 20 experiments were performed for each material, providing a comprehensive dataset for statistical analysis and model validation. **Result and discussion.** The results of the study highlight the effectiveness of numerical simulation in predicting the wear resistance of PTFE-based composites under dry sliding friction conditions. Experimental investigations reveal that pure PTFE exhibits low mechanical strength, leading to a high wear rate, whereas PTFE with carbon and glass fillers demonstrates improved wear resistance characteristics. The addition of carbon to PTFE enhances the composite's performance by forming a stable transfer film on the counterbody, while the addition of glass promotes increased hardness and, consequently, reduced material loss. Empirical models developed using response surface methodology (RSM) confirm that the applied load on the pin is the most significant parameter affecting wear, followed by sliding speed and temperature. Numerical simulations based on Archard's wear model exhibit good agreement with experimental data, validating the accuracy of the numerical simulations. This research contributes to a deeper understanding of the application of PTFE-based composites in extending the service life and enhancing the reliability of industrial products.

**For citation:** Deshpande A., Kulkarni A.P., Anerao P., Deshpande L., Somatkar A. Integrated numerical and experimental investigation of tribological performance of PTFE based composite material. *Obrabotka metallov (tekhnologiya, oborudovanie, instrumenty) = Metal Working and Material Science*, 2025, vol. 27, no. 2, pp. 219–237. DOI: 10.17212/1994-6309-2025-27.2-219-237. (In Russian).

Kulkarni Atul P., Professor  
 Vishwakarma Institute of Technology,  
 Pune, Maharashtra, 411037, India

Tel.: (+91) 9922914460, e-mail: [atul.kulkarni@vit.edu](mailto:atul.kulkarni@vit.edu)

## Introduction

Polymers have recently replaced metals in tribological applications because of their numerous advantages, including self-lubrication, chemical stability, low density, and biocompatibility. This transformation in tribo-system components has increased the demand for the development of high-performance and cost-effective polymer composites. PTFE has emerged as a most prominent choice for applications such as mining, automotive, aerospace, electrical, and electronics industries [1]. With its unique combination of properties, such as a low coefficient of friction, exceptional chemical inertness, high thermal stability, and non-stick characteristics, *PTFE* effectively minimizes friction and wear by establishing a thin transfer film on the contacting surface. This ability of *PTFE*, along with its thermal and chemical stability, makes it suitable for various industrial applications where wear performance is required [2]. However, pure *PTFE* alone cannot withstand the demands of tribological applications. Therefore, researchers have explored the addition of various fillers to reinforce pure *PTFE*, improving its mechanical and tribological performance. The most used fillers are carbon, glass, graphite, bronze,  $MoS_2$ , alumina, *PEEK* (polyetheretherketone), and potassium titanate whisker (*PTW*) [3]. The researchers also studied advanced fillers such as ekonol, polyether sulphone, and poly-p-phenyleneterephthalamide (*PPDT*) fibers for their potential benefits [4].

Carbon is a widely used filler because it increases the wear resistance of the base material and significantly increases the tensile strength, impact strength, and hardness [3]. This improvement of *PTFE* properties is achieved with the incorporation of carbon at a concentration of 15 to 30 % by volume [4]. The addition of carbon makes *PTFE* more suitable for high load and temperature applications. Glass, when added to *PTFE*, enhances hardness and tensile strength, improving the load-carrying capacity and wear resistance of the base material [5]. It also provides resistance to deformation and dimensional stability under high load and temperature conditions [6]. This ensures the improved performance of glass-filled *PTFE* composites in applications like bearings, seals, gaskets, and guide rails etc. [7]. Similarly, the load-bearing capacity, thermal stability, and wear resistance of *PTFE* are found to be improved with the addition of bronze at a concentration of 40 to 60 % by volume [8]. Researchers observed that the addition of bronze to *PTFE* provides stable frictional behavior and extends the service life of the components in applications such as seals, bearings, and bushings [9–10]. Further improvement in composite properties is achieved by adding molybdenum disulfide ( $MoS_2$ ) at a concentration of 5 % by volume, making it a promising candidate for automotive applications [11–13].

It is reported that the performance of polymer composites is influenced by several operating parameters, such as normal load, contact area, sliding speed, counterpart topology, and temperature [14–18]. These parameters are responsible for the formation of a stable film on the counterpart, which reduces the surface interaction, and eventually reduces the wear [19]. Similarly, few parameters (temperature and load) initiate the degradation of the composites and affect its behavior under certain conditions. Hence, it is required to study these parameters, and they shall be optimized to improve the performance of the composite [20]. It is also evident that these parameters affect the fundamental adhesion phenomenon of polymer composites, which affects its wear behavior.

Tribological study has traditionally employed experimental methods to evaluate wear and friction in materials. However, these studies are time-consuming, resource-intensive, and often possess constraints regarding identifying factors influencing wear mechanisms. Numerical modelling, particularly finite element analysis (*FEA*) in conjunction with *Archard's* wear model, has emerged as an efficient way to supplement experimental research [21]. These models allow researchers to simulate the wear process, predict the outcome under various operating circumstances, and optimize material design before physical testing. It is evident that *FEA* is an extremely versatile and powerful tool for wear simulation. Under dynamic load and environmental conditions, *FEA* provides comprehensive analysis of stress distribution, deformation, and wear development [22]. It enables researchers to investigate local wear phenomena and understand the wear mechanism in greater detail. The studies reflect that the predictive capabilities of the wear model are improved by combining *Archard's* law with *FEA* [23–24]. In the present study, a numerical approach has been considered based on the *Archard* model, and the results are validated using experimental analysis. The

tribological behaviour of three composite materials - pure *PTFE* (*M1*), *PTFE* with 25 % carbon (*M2*), and *PTFE* with 20 % glass fibre (*M3*) - was investigated as a function of operating parameters such as load, sliding speed, and temperature. The study also aims to evaluate the predictive capability of the proposed numerical model for wear analysis.

## Materials and Methods

### Materials

The samples were manufactured using compression molding and procured from *Innominds Engineering*, Pune, Maharashtra. The specimens were machined to a radius of 5 mm and a length of 32 mm using a *SimpleTurn 5075 CNC* machine procured from *ACE Micromatic*, Bangalore, India. The actual test specimens are shown in Fig. 1. The *PTFE* composite properties are given in Table 1. Typically, the volume fraction of carbon in *PTFE* ranges from 10 % to 30 %, depending on different industrial applications. However, a 25 % volume fraction of carbon was considered for the present study, as it provides considerable mechanical reinforcement as well as better stiffness and strength to *PTFE* [9]. It also avoids agglomeration of the filler, prevents overloading, and provides thermal stability, which improves the wear behavior of the material. Similarly, glass at a 20 % volume fraction in *PTFE* provides dimensional stability by reducing creep and deformation under load. Furthermore, glass additionally provides chemical stability to *PTFE*, making it effective for corrosive environments [16].

Table 1

Properties of *PTFE*-based composite

Properties	ASTM Code	<i>M1</i>	<i>M2</i>	<i>M3</i>
Density ( $\text{kg/m}^3$ )	ASTM D 792 [16]	2,160	2,244	2,147
Tensile Strength (MPa)	ASTM D 638 [16]	22.7	15.54	15.8
Compressive Strength (MPa)	ASTM D 638 [16]	4.32	15.46	14.32
Shore D Hardness	ASTM D 2240 [16]	49	65	61



*a*



*b*



*c*

Fig. 1. Test specimen (a) *M1*, (b) *M2* and (c) *M3*

### Experimental Details

Tribological tests were conducted using a pin-on-disc tribometer (*Ducom Instruments Pvt. Ltd.*, Bangalore, India). The operating principle of the setup involves rotating a disc at a constant speed while maintaining a stationary pin pressed against the disc with a specified load. Wear is initiated due to the relative motion between the pin and the disc. The disc is made of austenitic stainless steel (*SS 304*) with a 165 mm diameter and 8 mm thickness. The average hardness of the plate across the surface was found to be 58 HRC, and the average surface roughness was 1.8  $\mu\text{m}$ . A linear variable differential transducer (*LVDT*)

was used to record the displacement of the pin, which is correlated to measure the wear of the material. Additional attachments, such as a pin heater and environmental chamber, are provided for conducting experiments that simulate actual working conditions. Fig. 2 shows the complete experimental setup of the pin-on-disc tribometer. Figs. 2, *a–c* depict the attachments for pin heating, the testing setup, and the controller with software, respectively. The setup specifications allow for testing within a load range of 0 N to 200 N and a rotational speed range of 200 rpm to 2000 rpm. The pin diameter can range from 3 mm to 10 mm. The accuracy of the *LVDT* is  $\pm 1\%$  of the measured wear in  $\mu\text{m}$ , and the least count is  $1\ \mu\text{m}$ , which helps to measure wear from  $3\ \mu\text{m}$  to  $1,200\ \mu\text{m}$ . The heating temperature can be raised up to  $400\ ^\circ\text{C}$ . The wear track diameter varies from 55 mm to 154 mm. In the present study, it is held constant at 100 mm.

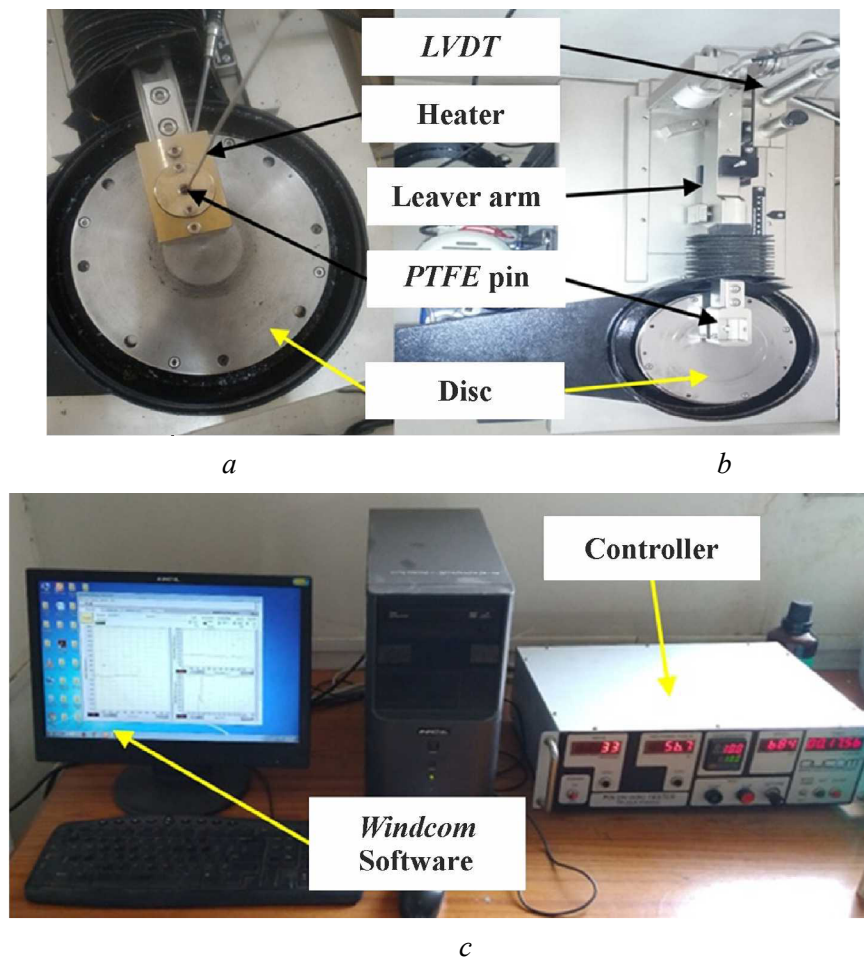


Fig. 2. Pin-on-disc tribometer (a) pin heater, (b) experiment setup and (c) controller and *Windcom* software

A suitable track diameter was selected corresponding to the disk rotation to finalize sliding velocities according to the *CCRD* (central composite rotatable design) experiment framework. This experimental design provides consistent prediction variance at equidistant points from the center of the design space. *CCRD* allows the input variable levels to be determined by using an alpha value calculated using  $(2^K) \times 0.25$ , where  $K$  is the number of input variables. In the present study, three variables (pressure, rotational speed, and temperature) were considered, which results in an alpha value of  $\pm 1.682$ . Initially, the minimum and maximum range of variables was established based on actual working constraints and assigned values of  $-1.682$  and  $+1.682$ , respectively. The intermediate levels were determined using linear interpolation and a linear equation ( $\text{Alpha value} = a + b \times \text{variable value}$ ). These derived intermediate levels ensure even distribution within the minimum and maximum range. Table 2 shows the levels of parameters selected for the experimentation, and Table 3 shows the alpha values and corresponding intermediate levels of the variables.

Table 2

**Levels of parameters for the experiments**

Parameters	Normal load (N)	Sliding Speed (rpm)	Temperature (°C)
Low level	15	400	60
High level	200	1,000	200
Track Distance 5 km			

Table 3

**Alpha values and corresponding variable levels**

Alpha Value	−1.682	−1	0	+1	+1.682
Normal load (N)	15	55	115	155	200
Sliding Speed (rpm)	400	521	700	878	1,000
Temperature (°C)	60	88	130	171	200

Table 4 shows the experimental matrix. The trials were conducted for all specimens at a constant sliding distance of 5 km, and 20 experiments were conducted for each specimen material. It is evident from the experimental matrix that experiments 15–20 represent repetitions of the center point. Researchers can assess

Table 4

**Experimental matrix**

Run	Normal load (N)	Sliding speed (rpm)	Temperature (°C)
1	55	521	88
2	155	521	88
3	55	878	88
4	155	878	88
5	55	521	172
6	155	521	172
7	55	878	172
8	155	878	172
9	15	700	130
10	200	700	130
11	115	400	130
12	115	1000	130
13	115	700	60
14	115	700	200
15	115	700	130
16	115	700	130
17	115	700	130
18	115	700	130
19	115	700	130
20	115	700	130



the inherent variability in their measurements using these repetitions of the center point experiments. This helps in accounting for experimental error introduced due to uncontrollable factors, such as environmental conditions. These experiments quantify the error, which is essential for evaluating the statistical significance of the findings. The consistency of the center point repetitions strengthens confidence in the predictive capabilities of the model.

### Numerical Approach

The workflow for simulating the tribological analysis of a *PTFE* composite using a pin-on-disc setup with *FEA* is shown in Fig. 3. The pin-on-disc setup model was generated in *SOLIDWORKS*, followed by simulation using *ANSYS 2021 R2 Workbench*. The properties of the corresponding materials were imported into *FEA* to accurately simulate the model, which provides reliability in the prediction ability of the model. In *ANSYS Workbench*, the disc and pin were assigned frictional contact with asymmetric behavior, and their motion was restricted to specific degrees of freedom by assigning them ground joints [21]. The disc was modeled as a rigid body, whereas the pin was treated as a flexible body to incorporate its deformation. A translation joint was assigned to the pin in the vertical direction; however, the disc was assigned a revolute joint. The detection method was set to nodal normal to the target, aligning with the applied force on the pin. Similarly, the trim contact was disabled to allow for aggressive stiffness updates, which helped to accelerate convergence and reduce simulation time. Meshing was performed using the auto-meshing capabilities of *ANSYS Mechanical APDL*. The 3D elements were meshed with a combination of tetrahedral and hexahedral elements. The tetrahedral elements easily conform to the complex geometry, whereas hexahedral elements are used in regular shapes for better accuracy [22]. Analysis settings were configured, and *Archard's* wear model was incorporated, defining its wear coefficient ( $K$ ) as  $0.988 \times 10^{-4}$  to predict the volume loss.

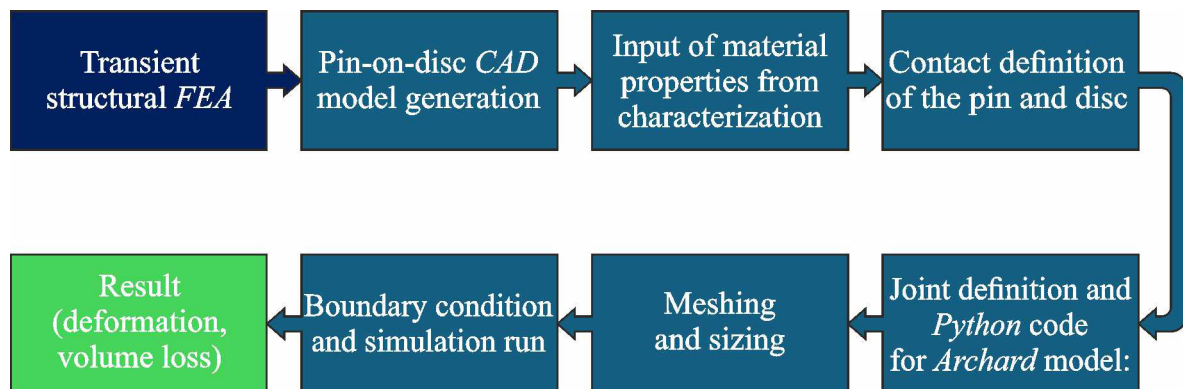


Fig. 3. Flow chart of numerical simulation

*Archard's* wear law establishes the wear rate as a linear function of the applied load, sliding speed, softer material hardness, and wear coefficient. However, this law focuses mainly on contact surfaces and ignores the effect of surface roughness or duration of the run. *ANSYS Workbench* was employed to model the *FEA* modeling of the pin-on-disc arrangement for simulation. Transient structural analysis was performed by providing the respective properties of the disc and pin material. Initially, sample trials were performed and validated with the experimental results.

### Power law

In tribo-systems, the behaviour of materials under different operating conditions can be effectively captured by using a power law. The relationship between dependent variables, such as wear and coefficient of friction, and independent variables, such as sliding speed, load, and temperature, is defined for predictive analysis. It is expressed as:

$$y = ax^k, \quad (1)$$

where  $x$  and  $y$  are independent and dependent variables, respectively;  $a$  is the proportionality constant;  $k$  is the power exponent.

It is observed that tribological studies in adhesive wear conditions show power law behavior, where small variations in a parameter significantly influence the dependent parameter. This helps in identifying the dependency of the wear rate on different operating variables, making the power law useful for designing components with better performance. The power law offers a robust approach to understanding wear and friction of materials, making it a significant tool in tribological applications [24]. It also helps in preventing premature failure, designing durable materials, and optimizing operating parameters. However, its limitations need to be analyzed, and assumptions need to be validated with empirical data.

## Results and Discussion

A pin-on-disc setup was used for experimentation with a fixed sliding distance of 5 km. Fig. 4 shows the track image along with the track impression on the SS 304 plate.

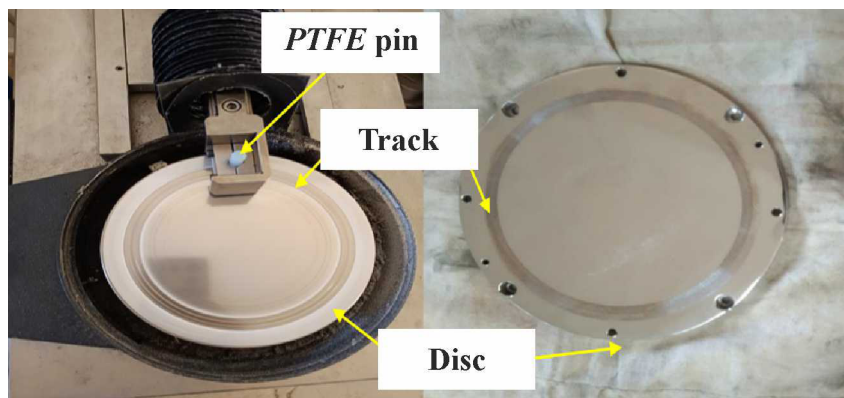


Fig. 4. Track image of pins on SS 304 steel disc

Before starting the experiments, the weight of each specimen was recorded, and experiments were performed as per the DoE. The mass loss was recorded for different normal loads, sliding speeds, and temperatures. Volume loss and specific wear rate for each condition were determined using Equation 2 and Equation 3.

$$\text{Volume loss (mm}^3\text{)} = \frac{\text{Mass loss (m)}}{\text{Density } (\rho)} \quad (2)$$

$$\text{Sp. wear rate (mm}^3 / \text{N} \times \text{m)} = \frac{\text{Volume loss (mm}^3\text{)}}{\text{Load (N)} \times \text{Sliding distance (m)}} \quad (3)$$

The experimental results for all the trials are tabulated in Table 5.

A mathematical equation based on the power law was considered to predict wear by considering the normal load (N) and speed (RPM), and it is given in Equation 4. Generally, the power law is used to understand the influence of multiple input parameters on the output response.

$$W = a \times L^b \times S^c \times T^d, \quad (4)$$

where  $W$  is the specific wear rate;  $L$  is the normal load;  $S$  is the sliding speed;  $T$  is the temperature;  $a$ ,  $b$ ,  $c$  and  $d$  are the constants.

The values of these constants were determined for materials  $M1$ ,  $M2$ , and  $M3$  using experimental data. *DataFit* software was used to obtain the correlation between wear, normal load, sliding speed, and temperature; the empirical equation for the corresponding material is given in Table 6.

The majority of test runs showed that  $M2$  exhibits better wear resistance, characterized by the lowest volume loss and specific wear rate. At a load of 2 N and a speed of 400 rpm,  $M2$  gave a volume loss

Table 5

### Experimental results for material *M1*, *M2* and *M3*

Run	<i>M1</i>		<i>M2</i>		<i>M3</i>	
	Volume loss (mm <sup>3</sup> )	Specific wear rate (mm <sup>3</sup> /N·m)	Volume loss (mm <sup>3</sup> )	Specific wear rate (mm <sup>3</sup> /N·m)	Volume loss (mm <sup>3</sup> )	Specific wear rate (mm <sup>3</sup> /N·m)
1	13.0605	4.749E-05	1.6042	9.3125E-06	10.0141	3.641E-05
2	85.0757	1.098E-04	9.7269	2.0036E-05	53.2009	6.865E-05
3	24.7405	8.997E-05	2.8127	1.6328E-05	20.3713	7.408E-05
4	155.9154	2.012E-04	18.0080	3.7094E-05	109.5102	1.413E-04
5	16.3985	5.963E-05	1.9445	1.1288E-05	12.2503	4.455E-05
6	101.9721	1.316E-04	10.7772	2.2200E-05	64.0694	8.267E-05
7	26.6520	9.692E-05	3.1404	1.8230E-05	24.6040	8.947E-05
8	185.1592	2.389E-04	18.0080	3.7094E-05	123.9012	1.599E-04
9	2.2919	3.056E-05	0.4156	8.8462E-06	2.2741	3.032E-05
10	216.3670	2.164E-04	19.4754	3.1091E-05	128.4902	1.285E-04
11	35.4290	6.162E-05	4.2400	1.1772E-05	25.7003	4.470E-05
12	107.6915	1.873E-04	12.8762	3.5749E-05	78.6877	1.368E-04
13	55.6731	9.682E-05	6.5551	1.8199E-05	43.8375	7.624E-05
14	82.5310	1.435E-04	8.2850	2.3002E-05	59.2238	1.030E-04
15	70.8319	1.232E-04	8.1029	2.2496E-05	50.6657	8.811E-05
16	72.9259	1.268E-04	7.5111	2.0853E-05	50.0740	8.709E-05
17	68.1916	1.186E-04	6.6007	1.8326E-05	48.0710	8.360E-05
18	71.8334	1.249E-04	7.2835	2.0222E-05	50.2105	8.732E-05
19	70.3767	1.224E-04	7.7842	2.1612E-05	52.1680	9.073E-05
20	78.7527	1.370E-04	7.6477	2.1233E-05	49.4367	8.598E-05

Table 6

### Empirical equation for each material

Material	Equation
<i>M1</i>	$W = (2.74E - 10) \times L^{0.874} \times S^{1.155} \times T^{0.277}$
<i>M2</i>	$W = (1.02E - 10) \times L^{0.672} \times S^{1.231} \times T^{0.216}$
<i>M3</i>	$W = (3.58E - 10) \times L^{0.598} \times S^{0.598} \times T^{0.232}$

of 1.6042 mm<sup>3</sup> with a specific wear rate of 9.3125E-06 mm<sup>3</sup>/N×m compared to volume losses of *M1* (13.0605 mm<sup>3</sup>) and *M3* (10.0141 mm<sup>3</sup>).

Material *M2* performed better than *M1* and *M3* when the load and speed were incremented. At a 25 N load and 1,000 rpm, *M1* showed the highest volume loss of 185.1592 mm<sup>3</sup>, followed by material *M3*, which showed a volume loss of 123.9012 mm<sup>3</sup>. Meanwhile, *M2* showed the lowest volume loss of 18.0080 mm<sup>3</sup> with a specific wear rate of 3.7094E-05 mm<sup>3</sup>/N×m.

The consistency of the data obtained from the center point replicates (Runs 15-20) validates the reproducibility of the experimental methodology. The average specific wear rate of *M2* at the center point was 2.108E-05 mm<sup>3</sup>/N×m, lower than that of *M1* (1.238E-04 mm<sup>3</sup>/Nm) and *M3* (8.814E-05 mm<sup>3</sup>/Nm).

The value of the correlation coefficient (*R*<sup>2</sup> value) obtained was 0.91, 0.96, and 0.93, indicating that the empirical expression developed (shown in Table 6) would be effectively suitable to understand the wear



rate of  $M1$ ,  $M2$ , and  $M3$  against  $SS\ 304$  stainless steel in the range of parameters selected in this study. The exponents of the empirical relations clearly indicate that material  $M1$  shows a linear relationship with load as well as temperature; however, material  $M3$  shows a dependency on the sliding velocity. Material  $M1$  under higher load and temperature showed higher wear, limiting its use for higher loading conditions. Whereas material  $M3$  was least resistant to wear due to its higher pre-factor as well as higher exponents for sliding velocity and temperature. Material  $M2$  showed lower sensitivity towards load and temperature as well as moderate sensitivity to sliding velocity, emerging as an overall wear-resistant material.

The 3-D plots reflecting the variation in the specific wear rate are shown in Figs. 5, 6, and 7, *a-c*) for materials  $M1$ ,  $M2$ , and  $M3$ , respectively. The plot shown in Fig. 5, *a* indicates that the specific wear rate shows a strong dependency on load and sliding velocity. However, the specific wear shows a steeper slope with load compared to sliding velocity, indicating a considerable impact of load on the wear rate for material  $M1$ . In Fig. 5, *b*, the contours show that specific wear is rapidly influenced by the load rather than temperature, indicating the dominant role of load in determining the specific wear rate for the tested conditions of parameters. The plot shown in Fig. 5, *c* shows a steeper gradient along the sliding velocity than temperature. It clearly indicates that sliding velocity has a slightly higher influence on the wear behavior of material  $M1$  than the temperature.

Figs. 6, *a, b* and *c* show the performance of material  $M2$  under load, temperature, and sliding velocity. At higher values of the parameters, the frictional force and the interface temperature increase, resulting in surface degradation; hence, a noticeable rise in wear is observed. Higher temperatures and loads accelerate material wear by reducing its resistance to deformation, as the matrix material softens, leading to increased wear. Additionally, wear tends to increase with a rise in sliding velocity due to greater heat generation at the interacting surfaces. The effect becomes even more pronounced as the temperature continues to rise.

The surface plots in Figs. 7, *a, b* and *c* illustrate the behavior of material  $M3$  under different operating conditions. It is evident that the wear rate follows a non-linear trend concerning these parameters. Higher loads increase stress in the contact region, leading to greater wear, even at lower sliding velocities and temperatures. Increased sliding velocity causes thermal degradation of the material, further accelerating

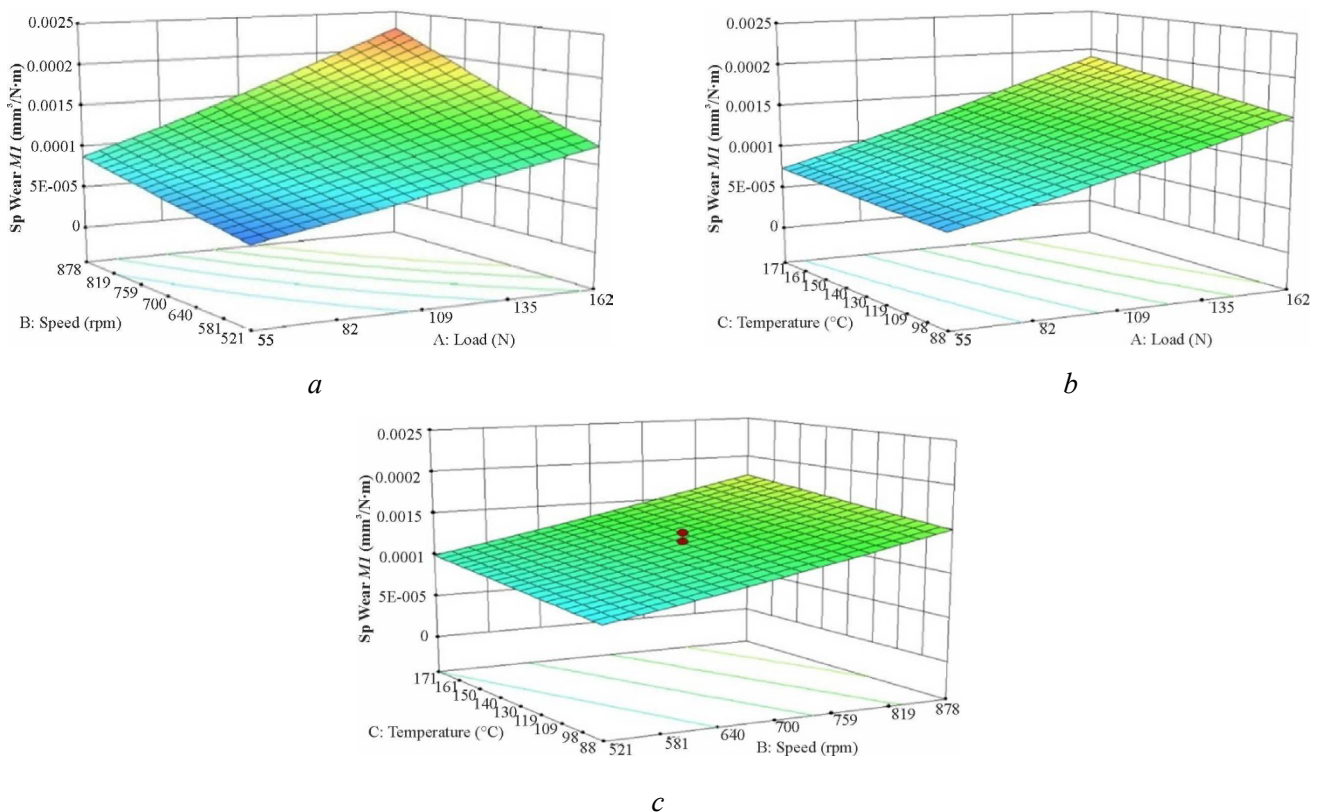


Fig. 5. Specific wear rate for  $M1$  (*a*) normal load vs sliding speed, (*b*) normal load vs temperature and (*c*) sliding speed vs temperature

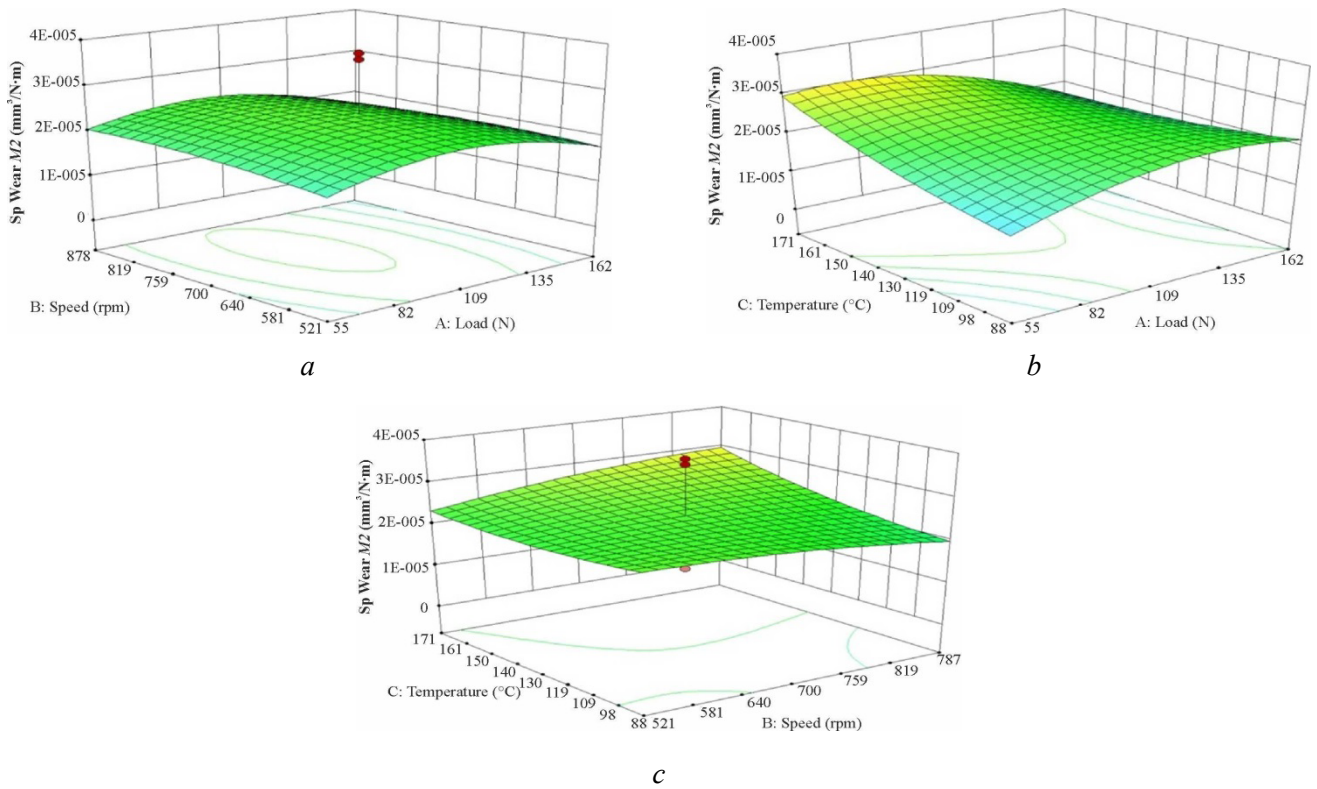


Fig. 6. Specific wear rate for M2 (a) normal load vs sliding speed, (b) normal load vs temperature and (c) sliding speed vs temperature

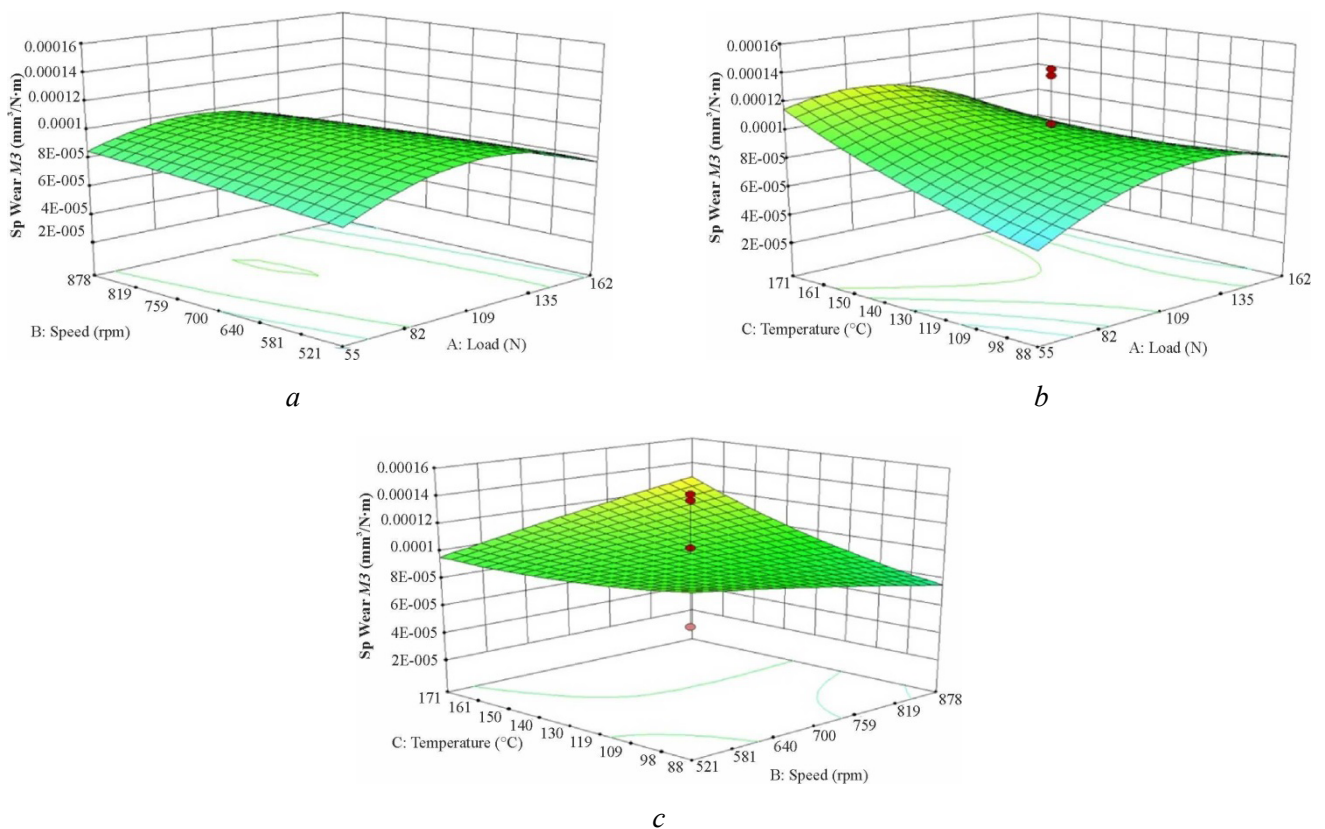


Fig. 7. Specific wear rate for M3 (a) normal load vs sliding speed, (b) normal load vs temperature and (c) sliding speed vs temperature

wear. Similarly, elevated temperature results in thermal softening, which contributes to increased wear. However, the wear rate remains stable within a moderate range of operating parameters.

Fig. 8, *a* represents the effect of load on the specific wear rate at a constant temperature of 130 °C and a speed of 700 rpm. It is observed that material *M1* has insufficient reinforcement against the wear and is sensitive to the interface pressure; hence, it shows a sharp increase in wear at higher loading conditions. However, the better load-bearing capacity of material *M2* makes it perform effectively under different loading conditions. Similarly, material *M2* shows thermal stability due to its reinforcement against the temperature variations. However, due to thermal softening, material *M1* degrades and shows poor performance against the temperature. Material *M2* also shows effective resistance to variations in the speed. It is clarified that material *M3* performs moderately against the different operating conditions.

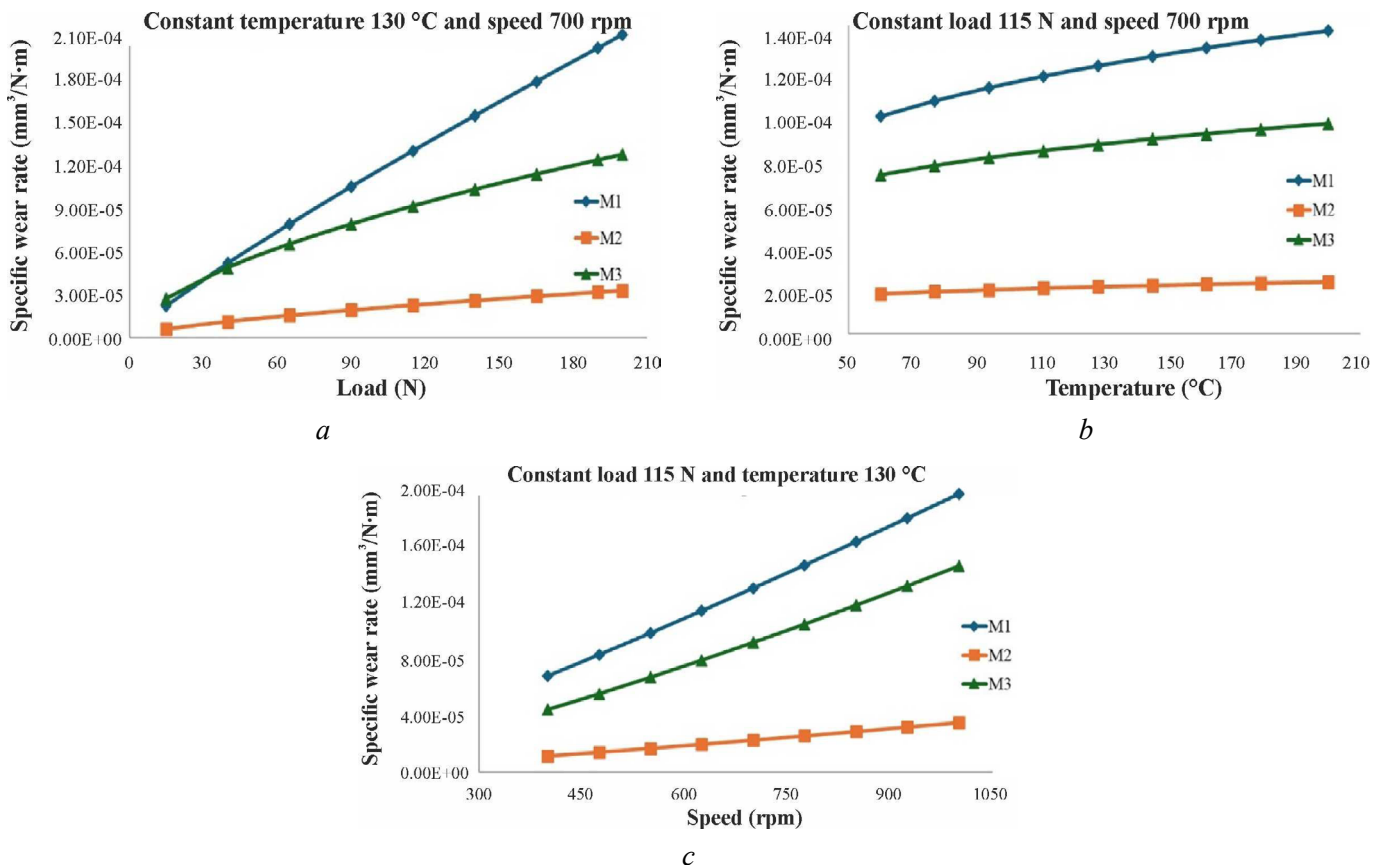


Fig. 8. Specific wear rate (*a*) constant temperature 130 °C and speed 700 rpm (*b*) constant load 115 N and speed 700 rpm and (*c*) constant load 115 N and temperature 130 °C

*Archard's* wear model is integrated with finite element analysis simulation using a volume probe to determine the incremental wear. *Archard's* wear model principally calculates the wear volume based on the contact region, overall sliding distance, and stress distribution, while *FEA* estimates the volume loss based on the surface interactions. The volume probe, a more refined approach, estimates the wear volume, taking into consideration the local variations in the contact conditions such as coefficient of friction and hardness. This enhances the predictive ability of the simulation model. Fig. 9, *a* represents a typical pin-on-disc arrangement, which is widely used to study wear behavior under controlled operating conditions. The disc, modeled as a rigid body, is assigned a revolute joint, whereas the flexible body pin is given a translation motion in a vertical direction along the disc. Fig. 9, *b* shows refined meshing near the contact region of the pin and disc to obtain accurate deformation and stresses to ensure computational accuracy of the model. Fig. 9, *c* represents the pressure distribution on the disc under transient structural loading conditions. The load is effectively distributed between the pin and the disc at the contact region. The pin surface is subjected to effective deformation under the concentrated loading condition, as shown in Fig. 9, *d*.



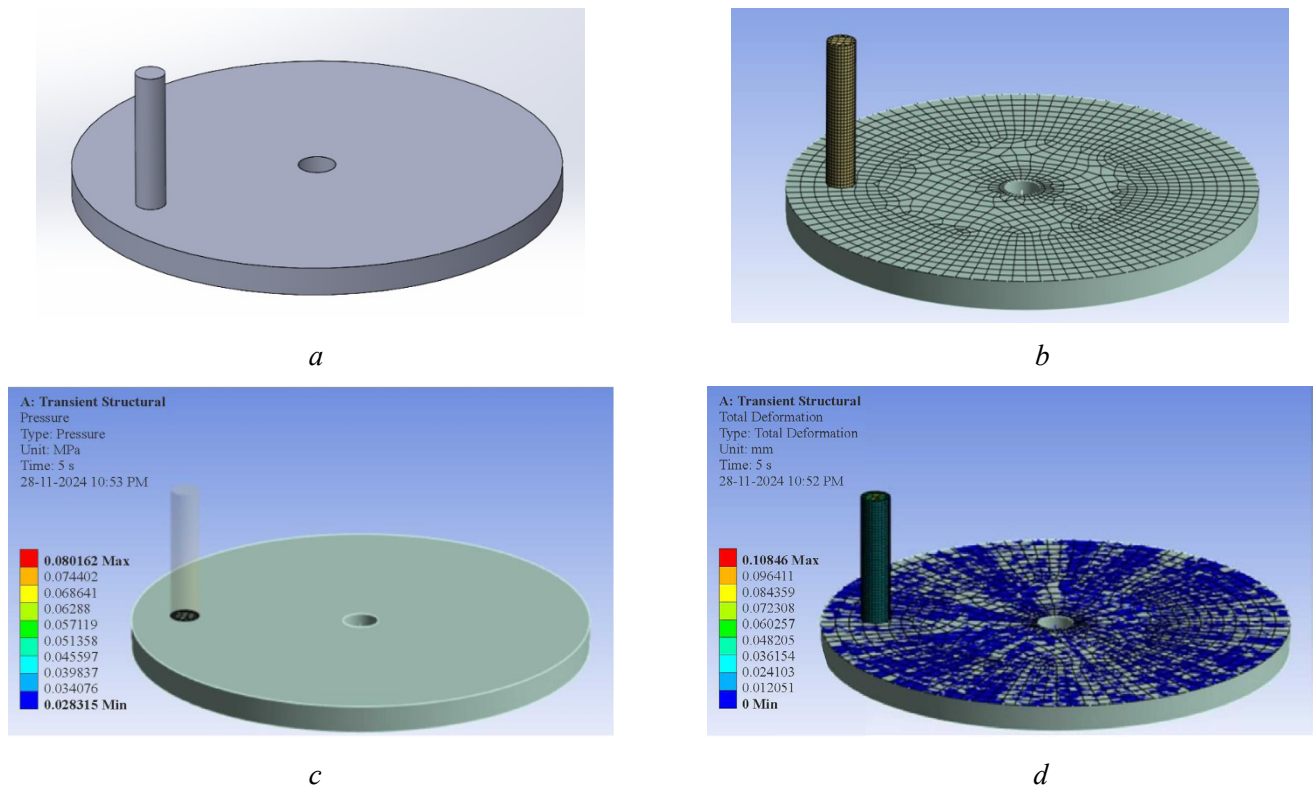


Fig. 9. FEA analysis:

*a* – modelling; *b* – meshing; *c* – pressure distribution; *d* – simulation

Material *M1* showed moderate agreement between experimental and numerical results, as shown in Fig. 10, *a*. However, it was observed that higher loading conditions showed considerable deviation in the results. In Fig. 10, *b*, material *M2* showed closer agreement between experimental and numerical results. It was also observed that the simulation model overestimated the volume loss compared to the experimental results; however, the results were found to be more consistent. Fig. 10, *c* shows that, for material *M3*, the simulation model consistently overestimated the volume loss. It was observed from the results that material *M2* outperformed materials *M1* and *M3*, as predictions aligned closely with the experimental results. The deviation in the results might have been observed due to factors such as material inhomogeneity, surface conditions, and external environmental factors, which the simulation model failed to address.

## Conclusions

This study focuses on the tribological performance evaluation of three materials - *M1*, *M2*, and *M3* - under different operating conditions using experimental, statistical, and numerical approaches. It was observed that *M1* exhibited the highest wear rate under high load and temperature situations, whereas *M2* showed moderate wear resistance. *M2* offers superior wear resistance, thermal stability, and low sensitivity to different operating conditions. The amalgamation of experimental and numerical approaches gives a robust framework for evaluating and predicting the tribological behaviour of the composite materials. This provides a pathway to overcome the time and resource constraints of the experimental approach, with improved ability to predict the material performance with accuracy and reliability. The following conclusions can be derived from the present study:

- The experimental and numerical analysis revealed that 25 % carbon-filled *PTFE* (*M2*) outperformed pure *PTFE* (*M1*) and 20 % glass-filled *PTFE* (*M3*) in wear resistance under various operating conditions. *M2* exhibited the lowest specific wear rate of  $3.1091 \times 10^{-5} \text{ mm}^3/\text{N}\times\text{m}$  under high load (200 N), speed (700 rpm), and temperature (130 °C), significantly reducing wear by 93.6 % compared to *M1* and 71 % compared to *M3*.

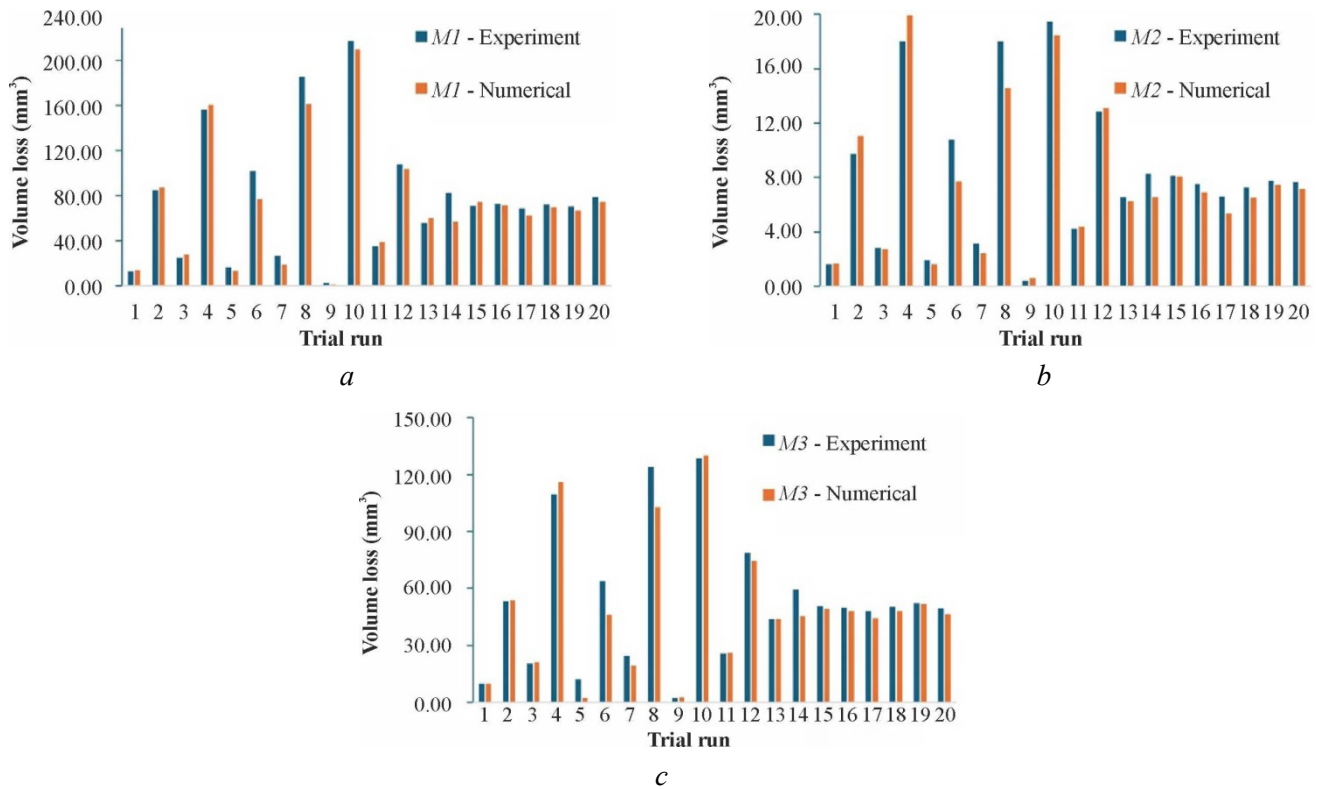


Fig. 10. Comparison between experimental and simulation results (a) material M1 (b) material M2 (c) material M3

– Numerical simulations using *Archard's* wear model closely aligned with experimental results, particularly for M2, with deviations of less than 10 % under moderate conditions. However, M3 showed a 10–15 % overestimation in wear predictions, while M1 displayed larger discrepancies due to its thermal softening under higher loads and temperatures, highlighting the importance of material reinforcement.

– Material M1, possessing the lowest wear resistance, exhibits high sensitivity to load and temperature due to its poor mechanical strength. Material M3 demonstrates moderate wear characteristics; however, its specific wear rate significantly exceeds that of M2 under extreme conditions. Material M2, characterized by superior load-bearing capacity, thermal stability, and consistent performance, is the most promising material for high-stress tribological applications. Optimization of operating parameters, involving maintaining a load of 160 N, a sliding speed of 451 rpm, and a temperature of 130 °C, minimizes wear and validates the effectiveness of empirical models for predicting the tribological behaviour of materials.

## References

1. Rojacz H., Maierhofer D., Piringer G. Environmental impact evaluation of wear protection materials. *Wear*, 2025, vol. 560–561, p. 205612. DOI: 10.1016/j.wear.2024.205612.
2. Holmberg K., Kivikytö-Reponen P., Härkisaari P., Valtonen K., Erdemir A. Global energy consumption due to friction and wear in the mining industry. *Tribology International*, 2017, vol. 115, pp. 116–139. DOI: 10.1016/j.triboint.2017.05.010.
3. Bhushan B., Wilcock D.F. Wear behavior of polymer compositions in dry reciprocating sliding. *Wear*, 1982, vol. 75 (1), pp. 41–70. DOI: 10.1016/0043-1648(82)90139-9.
4. Wang H., Feng X., Shi Y., Lu X. Effect of fibrous filler on friction on wear of PTFE composite under dry and wet condition. *China Particuology*, 2007, vol. 5 (6), pp. 414–419. DOI: 10.1016/j.cpart.2007.08.003.
5. Shangguan Q., Cheng X. Effect of rare earth on tribological properties of carbon fiber reinforced PTFE composites. *Journal of Rare Earths*, 2007, vol. 25, pp. 469–473. DOI: 10.1016/S1002-0721(07)60458-X.
6. Khedkar J., Negulescu I., Meletis E.I. Sliding wear behavior of PTFE composites. *Wear*, 2002, vol. 252 (5–6), pp. 361–369. DOI: 10.1016/S0043-1648(01)00859-6.



7. Mule R., Deshpande A., Verma U., Gumaste S., Kulkarni P., Shah J., Kulkarni A. A review on wear prediction models of polymers. *Transactions on Innovations in Science & Technology*, 2021, vol. 5 (2), pp. 278–282.
8. Satkar A.R., Mache A., Kulkarni A. Numerical investigation on perforation resistance of glass-carbon/epoxy hybrid composite laminate under ballistic impact. *Materials Today: Proceedings*, 2022, vol. 59 (1), pp. 734–741. DOI: 10.1016/j.matpr.2021.12.464.
9. Virpe K., Deshpande A., Kulkarni A. A review on tribological behavior of polymer composite impregnated with carbon fillers. *AIP Conference Proceedings*, 2020, vol. 2311, p. 070030. DOI: 10.1063/5.0035408.
10. Tevruz T. Tribological behaviours of bronze-filled polytetrafluoroethylene dry journal bearings. *Wear*, 1999, vol. 230 (1), pp. 61–69. DOI: 10.1016/S0043-1648(99)00091-5.
11. Mudasar Pasha B.A., Abdul Budan D., Basavarajappa S., Manjunath Yadav S., Nizamuddi B.A. Dry sliding wear behaviour of PTFE filled with glass and bronze particles. *Tribology – Materials, Surfaces & Interfaces*, 2011 vol. 5 (2), pp. 59–64. DOI: 10.1179/1751584X11Y.0000000006.
12. Venkateswarlu G., Sharada R., Bhagvanth Rao M. Effect of fillers on mechanical properties of PTFE based composites. *Archives of Applied Science Research*, 2015, vol. 7 (7), pp. 48–58.
13. Song F., Wang Q., Wang T. Effects of glass fiber and molybdenum disulfide on tribological behaviors and PV limit of chopped carbon fiber reinforced Polytetrafluoroethylene composites. *Tribology International*, 2016, vol. 104, pp. 392–401. DOI: 10.1016/j.triboint.2016.01.015.
14. Kolhe S., Deshpande A., Wangikar K. Wear behavior of Polytetrafluoroethylene composites: a review. *Smart technologies for energy, environment and sustainable development*. Singapore, Springer, 2019, pp. 571–584. DOI: 10.1007/978-981-13-6148-7\_55.
15. Kanitkar Y.M., Kulkarni A.P., Wangikar K.S. Characterization of glass hybrid composite: a review. *Materials Today: Proceedings*, 2017, vol. 4 (9), pp. 9627–9630. DOI: 10.1016/j.matpr.2017.06.237.
16. Deshpande A.R., Kulkarni A.P., Wasatkar N., Gajalkar V., Abdullah M. Prediction of wear rate of glass-filled PTFE composites based on machine learning approaches. *Polymers*, 2024, vol. 16 (18), pp. 2666. DOI: 10.3390/polym16182666.
17. Wang J., Chen B., Liu N., Han G., Yan F. Combined effects of fiber/matrix interface and water absorption on the tribological behaviors of water lubricated-polytetrafluoroethylene-based composites reinforced with carbon and basalt fibers. *Composites Part A: Applied Science and Manufacturing*, 2014, vol. 59, pp. 85–92. DOI: 10.1016/j.compositesa.2014.01.004.
18. Mu L., Feng X., Zhu J., Wang H., Sun Q., Shi Y., Lu X. Comparative study of tribological properties of different fibers reinforced PTFE/PEEK composites at elevated temperatures. *Tribology Transactions*, 2010, vol. 53 (2), pp. 189–194. DOI: 10.1080/10402000903097460.
19. Li F., Hu K., Li J., Zhao B. The friction and wear characteristics of nanometer ZnO filled polytetrafluoroethylene. *Wear*, 2001, vol. 249 (10–11), pp. 877–882. DOI: 10.1016/S0043-1648(01)00816-X.
20. Şahin Y. Analysis of abrasive wear behavior of PTFE composite using Taguchi's technique. *Cogent Engineering*, 2015, vol. 2 (1), pp. 1–15. DOI: 10.1080/23311916.2014.1000510.
21. Tabrizi A.T., Aghajani H., Saghaian H., Laleh F.F. Correction of Archard equation for wear behavior of modified pure titanium. *Tribology International*, 2021, vol. 155, p. 106772. DOI: 10.1016/j.triboint.2020.106772.
22. Hegadekatte V., Huber N., Kraft O. Finite element based simulation of dry sliding wear. *Modelling and Simulation in Materials Science and Engineering*, 2005, vol. 13, pp. 57–75. DOI: 10.1088/0965-0393/13/1/005.
23. Nile R., Verma U., Deshpande A., Joshi S., Shah J., Kulkarni A. Mathematical modeling of various forces acting on piston rod packing rings. *Materials Today: Proceedings*, 2022, vol. 49 (5), pp. 1521–1526. DOI: 10.1016/j.matpr.2021.07.304.
24. Kulkarni A.P., Chinchani S., Sargade V.G. Dimensional analysis and ANN simulation of chip-tool interface temperature during turning SS304. *Obrabotka metallov (tehnologiya, oborudovanie, instrumenty) = Metal Working and Material Science*, 2021, vol. 23 (4), pp. 47–64. DOI: 10.17212/1994-6309-2021-23.4-47-64.

## Conflicts of Interest

The authors declare no conflict of interest.